Parametric Uncertainty Identification and Model Reduction for Robust H_2 Synthesis for Track-Following in Dual-Stage Hard Disk Drives

Richard Conway, Sarah Felix and Roberto Horowitz

Computer Mechanics Laboratory

Mechanical Engineering

University of California, Berkeley, CA, USA

December 6, 2007

Abstract

This paper presents a systematic, semi-automated method for identifying parameters and parametric uncertainty for a set of dual-stage hard disk drives. A modal analysis technique is selected to extract parameters from a batch of frequency response data. In order to avoid redundancy in modal parameters, two methods are presented to reduce model order. One method combines experimental data to directly extract fewer parameters. The second method uses an optimized model truncation methodology. Finally, convex optimization and singular value decomposition are employed to obtain a minimally conservative, lower-order approximation of uncertain parameters. The result is a reduced-order state space model with parametric uncertainty to be used in robust H_2 control synthesis for a track-following hard disk drive servo.

Introduction

Increasing areal data densities in hard disk drives (HDDs) continue to motivate the development of high performance servo schemes for track-following control. Among the emerging configurations are dual-stage servos which incorporate a smaller-scale actuator onto the disk drive suspension in addition to the voice coil motor [1, 2]. It has also been shown that the use of optimal robust control synthesis techniques along with realistic disturbance models and modeling uncertainties results in dual-stage controllers with superior tracking performance [3].

A significant challenge in the implementation of control design techniques such as robust H_2 synthesis is the identification of model parameters and uncertainties. Minimizing conservatism in the uncertainty description can result in a controller with better performance. In addition, since robust H_2 synthesis optimizes over all the worst case combinations of the uncertain parameters, the computation time increases dramatically as the number of uncertain parameters increases. Thus, obtaining a description of the plant uncertainty with a minimal number of parameters is essential for posing a computationally feasible control design problem. This can be achieved through appropriate model reduction, and a minimal approximation of the uncertain set. The following presents systematic methods for each of these phases of system identification, originating from a set of experimental frequency response functions (FRFs). The methods are presented in the context of a hard disk drive application.

Model Identification

Model Form

Fig. 1 shows the experimental frequency response data for a batch of 15 dual-input, single-output hard disk drive plants obtained from [4]. The secondary input is piezoelectric (PZT) actuation of the suspension. Several distinct resonance modes are apparent in the data. It is therefore appropriate to represent the transfer function between the ith input and j^{th} output, $G_{ij}(s)$, as a summation of N modes, as follows:

$$G_{ij}(s) = \sum_{k=1}^{N} \left[\frac{b_0}{s^2 + \eta \omega_n s + \omega_n^2} \right]_{ij,k}. \tag{1}$$

This form requires only three parameters per mode: natural frequency, ω_n, damping coefficient, η , and modal constant, b_0. These parameters relate to insight about physical plant variations, which motivates the uncertainty analysis described in Section V.
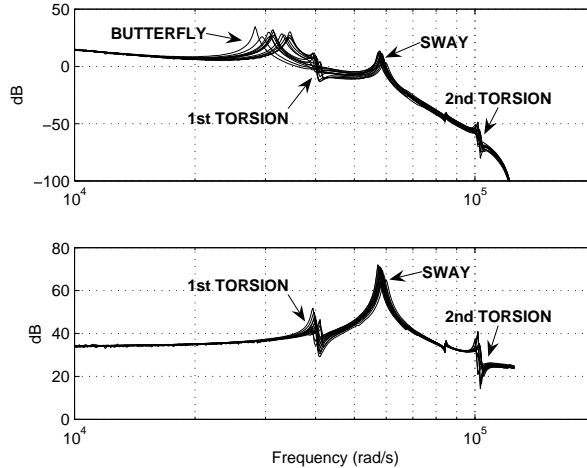
Figure 1: Experimental frequency response data from 15 dual-stage disk drives. Top: VCM to off-track displacement, bottom: PZT to off-track displacement.

Modal Parameter Identification

Parameters for each mode in the summation form are identified readily using single degree of freedom (SDOF) modal analysis. A SDOF model is based on the assumption that near a resonance frequency, the frequency response of a system is dominated by the dynamics of that resonance mode, and the contribution from other modes is a constant. This assumption is typically valid for disk drive structures [5], but should be verified by checking that the data points around each peak form a distinct ellipse when plotted in the Nyquist plane. In particular, when the FRF represents a displacement response and when the damping near each resonant frequency can be approximated by structural damping, as in $\bar{G}_{ij}(s)$ in (2), the ellipse is an exact circle [6].

$$\bar{G}_{ij}(s) = \sum_{k=1}^{N} \left[\frac{b_0}{s^2 + (\eta \omega_n^2/\omega)s + \omega_n^2} \right]_{ij,k} \tag{2}$$

This property is exploited for parameter identification, since ω_n, η, and b_0 can be extracted from the geometry of the circle, and a circle can be easily fit using a least squares algorithm. The equations for computing the modal parameters are derived from the complex function $\bar{G}_{ij}(j\omega)$ as in [6]. Fig. 2 illustrates a circle of data points in the Nyquist plane. The least squares fit determines the center of the circle and its radius, R.

The natural frequency is the frequency at which the sweep rate of data points around the circle, γ, is maximum, where γ is defined by

$$\gamma(\omega^2) = \frac{d\theta}{d(\omega^2)} \approx \frac{\Delta\theta}{\Delta(\omega^2)}. \tag{3}$$
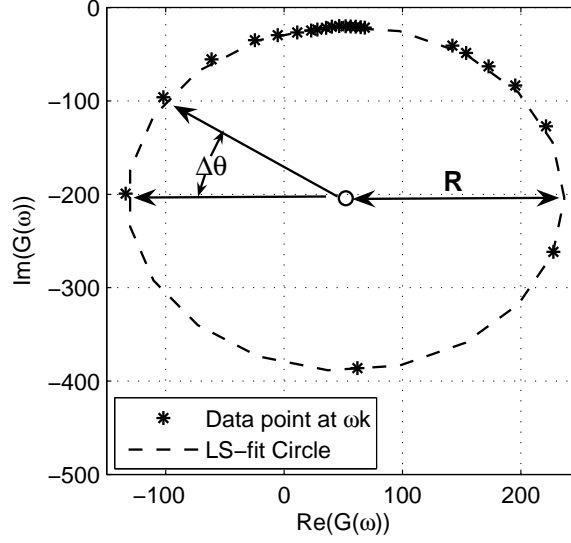
2

Figure 2: A least squares-based circle fit to the frequency response data points around the 1st torsion mode of the PZT response of one plant.

The remaining modal parameters are then given by the following equations:

$$\eta \;=\; \frac{2}{\omega_n^2 \gamma_{max}} \tag{4}$$

$$b_o \;=\; 2R\omega_n^2\eta. \tag{5}$$

It is clear in Fig. 2 that the resolution of the data points is poor, especially where sweep rate is at its maximum. This leads to significant error in the modal parameter estimates. A solution to this problem is to first fit some nominal curve, $F(s)$, to the experimental data, and then use this curve to pick off points of arbitrary density around the peak of each mode. $F(s)$ does not have to be constrained to the form in (1). It only has to provide an analytical transfer function that fits the data well. In some instances, the modal parameters can be extracted directly from $F(s)$. But it was found that this is not generally the case and the circle fit method is more robust.

This technique is used to obtain modal parameters from the FRFs for each plant in the batch. Fig. 3 shows a model fit to data points using the circle fit method. Five modes are identified in the VCM transfer function and three modes are identified in the PZT transfer function, for a total of sixteen states in the model. Finally, for each plant, the identified transfer functions are combined to form a multiple-input-multiple-output (MIMO) state space realization such that

$$G(s) = C(sI - A)^{-1}B. \tag{6}$$

3

It is possible that some modes may be considered negligible in the interest of limiting the model size. Thus, a priori knowledge is required from the designer about which modes are to be identified. In particular, the semi-automated circle fit algorithm developed requires that a frequency range be specified where each mode of interest is expected to appear in the FRF.

Model Reduction Via Data Fusion

It is evident in Figs. 1 and 3 that there are several modes that appear in both sets of FRFs, meaning both actuators excite some of the same modes in the structure. This leads to nearly redundant sets of eigenvalue pairs in the A matrix of the state space system, with slight differences being the result of error in measurements and parameter estimation. One way to avoid this redundancy is to simultaneously fit the data from the FRFs of all input-output pairs in order to extract common values for natural frequency and damping. Here, a method is proposed that combines the data at an intermediate step of the circle fitting algorithm. Further, the data is combined in a statistically meaningful manner by a weighted average based on variances. Once again, a design judgement is required to specify which modes are redundant.

As seen in (3)-(5), natural frequency and damping estimates both depend on γ_{max}. Further, common modes that occur in different FRFs will theoretically have the same $\gamma(\omega^2)$. As such, merging experimental data to get common values of $\gamma(\omega^2)$ is an efficient way to obtain common estimates of natural frequency and damping. Fig. 4 shows the sweep rate for a torsion mode in both the VCM response and the PZT response of a single plant. In the real data, there are differences in $\Delta\theta$ between the two data sets due to measurement and curve fitting error. Therefore, it makes sense to combine the sweep rate data using a weighted average based on the variance of each set of data. This weighted average is statistically justified using the principle of maximum likelihood, as in [8].

First, variance is characterized based on the error of the nominal curve fit, $F(s)$. Here, a least squares-based algorithm is used to compute $F(s)$, and it is assumed that the real and imaginary components of the error are Gaussian with zero mean and a covariance proportional to the identity matrix. In the Nyquist plane, this means that the components of the error in any rotated set of coordinates are also Gaussian and the second order statistics are preserved. Thus, the curve-fit error in $F(s)$ can be algebraically related to sweep rate. Consider the error between data point k and the value of $F(j\omega_k)$ at the corresponding frequency. Let e_k be the tangential component of this error relative to the Nyquist circle mapped from $F(s)$ and let ν be the variance of e_k. The estimate, $\hat{\gamma}(\omega^2)$, is then computed from a weighted average using the inverse of the variances of i data sets:
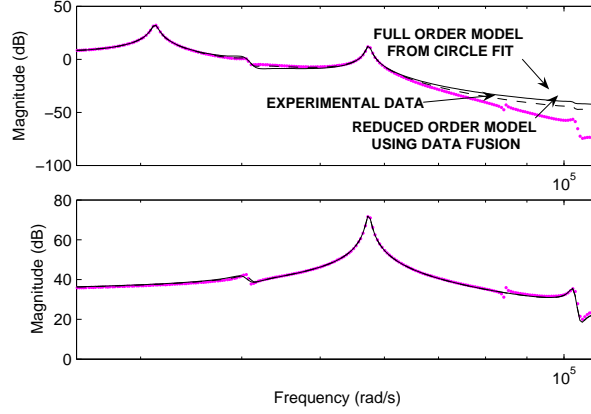
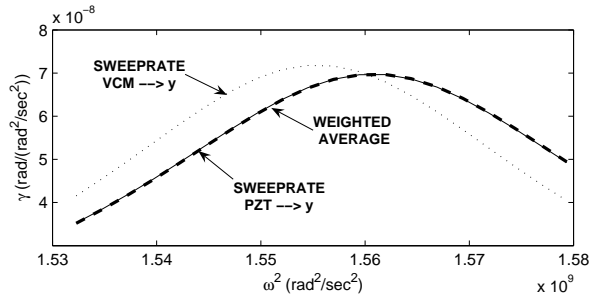Figure 3: Model from circle fit method with and without data fusion compared to data points for one plant

Figure 4: Angular sweep rate of FRF data points around the Nyquist plane circle for the 1st torsion mode

$$\hat{\gamma}(\omega^2) = \frac{\sum_i \gamma(\omega^2)/\nu_i}{\sum_i 1/\nu_i}. \tag{7}$$

Note that in this case, $i = \{1, 2\}$ since the estimate averages data from two input-output transfer functions. Fig. 4 shows $\hat{\gamma}(\omega^2)$ computed in this way. Note that it is heavily weighted toward the sweeprate from the PZT response. This is because the magnitude of the PZT response is much higher than that of the VCM response, so the relative tangential error is smaller. Once common estimates are obtained for natural frequency and damping coefficient, separate modal constants can be extracted from the circle radii of the individual data sets, as in (5). Fig. 3 shows the resulting model fit to the data. The new model is similar to the original model, but it has only ten states instead of sixteen states.

Model Reduction Via Optimized Truncation

The previous section discussed a method of directly consolidating experimental data to obtain common parameters. An alternative means of reducing the model order is to eliminate redundant eigenvalues in the MIMO state space realization using model reduction techniques. As a first step in this process, the order of
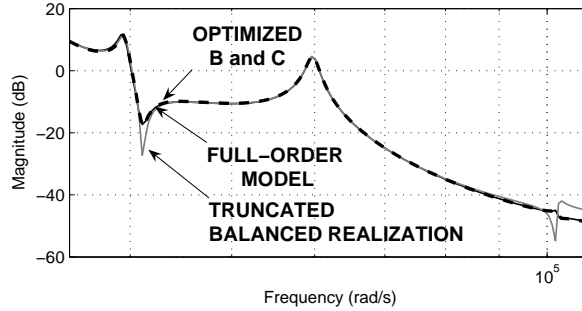
Figure 5: Bode magnitude plot of the displacement output response to VCM input showing full-order (16 state) and reduced-order (10 state) models

the model is reduced using balanced model truncation [8]. Because the repeated pairs of modes are weakly observable, balanced model truncation effectively eliminates the redundant eigenvalues in the A matrix. It is assumed here that the designer specifies either the number of redundant modes, or the threshold for truncation based on the Hankel singular values. Although a balanced model truncation is fast to compute and results in small additive H_∞ norm error [8], it is not optimal in any sense. In the case of the dual stage system, since the redundant modes are not necessarily weakly controllable, information is lost in the B and C matrices, resulting in significant error shown in Fig. 5. Notice that despite the error, the modes appear at the correct frequencies, indicating that the correct eigenvalues were preserved.

An additional optimization step improves the accuracy of the reduced-order system. This additional step is based on H_2 model reduction, which is currently a problem that can only be approximately solved using nonlinear, non-convex optimization [9]. The H_2 norm is used here because it corresponds to least squares in the frequency domain. As an alternative to finding a globally optimal reduced-order model, a method will be presented to refine the B and C matrices of the reduced-order model via H_2 model optimizations with closed-form solutions.

Let the state space realization of the reduced order model by given by

$$\hat{G}(s) = \hat{C}\left(sI - \hat{A}\right)^{-1}\hat{B} \tag{8}$$

For the full order plant and the reduced order plant, respectively define $G_{ij}(s)$ and $\hat{G}_{ij}(s)$ to be the single-input-single-output (SISO) transfer functions between the jth input and the ith output. Let $\overline{W}_{ij}(s)$ be a

stable, causal SISO weighting function between the jth input and the ith output. Then with the definitions

$$\overline{H}_{ij}(s) = \overline{W}_{ij}(s) \left[G_{ij}(s) - \hat{G}_{ij}(s) \right].$$
(9)

$$J_{mr} = \sum_{i=1}^{m} \sum_{j=1}^{n} \left\| \overline{H}_{ij}(s) \right\|_2^2$$
(10)

the optimization to be approximately solved is

$$\min_{\hat{B},\hat{C}} J_{mr}$$
(11)

Let $\overline{W}_{ij}(s)$ have the realization

$$\overline{W}_{ij}(s) \sim \left[\begin{array}{c|c} A_{ij}^W & B_{ij}^W \\ \hline C_{ij}^W & D_{ij}^W \end{array} \right].$$
(12)

Defining b_j to be the jth column of B, $\hat{b}_j$ to be the jth column to $\hat{B}$, c_i to be the ith row of C and $\hat{c}_i$ to be the ith row of $\hat{C}$, $H_{ij}(s)$ can be realized as

$$H_{ij}(s) \sim \left[\begin{array}{ccc|c} A_{ij}^W & B_{ij}^W c_i & -B_{ij}^W \hat{c}_i & 0 \\ 0 & A & 0 & b_j \\ 0 & 0 & \hat{A} & \hat{b}_j \\ \hline C_{ij}^W & D_{ij}^W c_i & -D_{ij}^W \hat{c}_i & 0 \end{array} \right]$$
$$= \left[\begin{array}{c|c} A_{ij}^H & B_{ij}^H \\ \hline C_{ij}^H & D_{ij}^H \end{array} \right].$$
(13)

Note that A_{ij}^H and C_{ij}^H are not functions of $\hat{B}$. Thus, with the assumption that $\hat{A}$ and $\hat{C}$ are known, it is possible to solve for the observability gramian, Q_{ij}, of $H_{ij}(s)$ by using the following Lyapunov equation:

$$\left(A_{ij}^H \right)^T Q_{ij} + Q_{ij} A_{ij}^H + \left(C_{ij}^H \right)^T C_{ij}^H = 0.$$
(14)

The H_2 norm of $H_{ij}(s)$ is then given by

$$\|H_{ij}(s)\|_2^2 = \left(B_{ij}^H \right)^T Q_{ij} B_{ij}^H,$$
(15)

which is quadratic in $\hat{b}_j$. The optimal values of the $\hat{b}_j$ vectors thus are given by

$$\hat{b}_j^o = -\left(Q_j^{33}\right)^{-1}\left(Q_j^{23}\right)^T b_j \tag{16}$$

where

$$\begin{bmatrix} Q_j^{11} & Q_j^{12} & Q_j^{13} \\ * & Q_j^{22} & Q_j^{23} \\ * & * & Q_j^{33} \end{bmatrix} = \sum_{i=1}^{m} Q_{ij} \tag{17}$$

Now note that when a system is transposed, the C matrix becomes the transpose of the B matrix. Since transposing $G(s)$ and $\hat{G}(s)$ and flipping the indices on the $W_{ij}(s)$ weighing functions does not change the problem, the problem of finding the optimal $\hat{C}$ while keeping $\hat{A}$ and $\hat{B}$ fixed is equivalent to finding the transpose of the optimal $\hat{B}$ matrix for the transposed systems. Although $\hat{B}$ and $\hat{C}$ cannot be optimized simultaneously using this methodology, they can be optimized one at a time in an alternating, iterative fashion until the model reduction cost, J_{mr}, converges.

Fig. 5 shows the Bode magnitude plot of the optimized reduced order model. Note that the optimized reduced order model is much more accurate than the initial reduced order system at frequencies close to the natural frequencies of the plant.

Uncertainty Approximation

Minimally Conservative Uncertainty Characterization

After a suitable reduced order model is obtained for each plant, the uncertainty in each parameter (e.g. ω_n) can be characterized. The vector of uncertain parameters, q, is represented as

$$q = \bar{q} + M\delta, \qquad \|\delta\|_\infty \leq 1 \tag{18}$$

where $\bar{q}$ represents the vector of nominal parameter values, δ is a vector of unknown real perturbations, and M is a square scaling matrix. Note that the jth reduced order model contains a value of the ith parameter, which will be denoted x_{ij}. Thus, for the jth reduced order plant, the measurement vector is defined as

$$v_j = \begin{bmatrix} x_{1j} & \cdots & x_{mj} \end{bmatrix}^T \tag{19}$$

It can now be seen that the characterization of the uncertain parameters requires the choice M and $\bar{q}$ such that each measurement vector can be described by a proper choice of δ.

Since the objective of robust controller design techniques is to design controllers that meet performance and/or robustness criteria for all $\|\delta\|_\infty \leq 1$, it is crucial to make M "small" so that the uncertainty description is minimally conservative. To quantify the size of M, the volume spanned by all feasible values of $M\delta$ will be used. Since minimizing the volume spanned by the set of feasible values of $M\delta$ is equivalent to minimizing the determinant of M, the problem to be solved is

$$\min_{M,\bar{q}} \det M \text{ subject to:}$$
$$\forall j \; \exists \delta^j : \left\|\delta^j\right\|_\infty \leq 1, \; \bar{q} + M\delta^j = v_j \tag{20}$$

The following are two approaches to solving this problem.

Scalar Characterization

If the uncertain parameters are assumed to have no coupling, i.e. M is a diagonal matrix, then the ith uncertain parameter, q_i, is represented as

$$q_i = \bar{q}_i + m_i \delta_i, \qquad |\delta_i| \leq 1 \tag{21}$$

The problem (20) can then be decoupled into a set of equivalent scalar optimizations which have closed-form solutions given by

$$\begin{bmatrix} \bar{q}_i^* \\ m_i^* \end{bmatrix} = \frac{1}{2} \begin{bmatrix} 1 & 1 \\ 1 & -1 \end{bmatrix} \begin{bmatrix} \max\{x_{i1}, \ldots, x_{in}\} \\ \min\{x_{i1}, \ldots, x_{in}\} \end{bmatrix} \tag{22}$$

Vectorial Characterization

Suppose now that the assumption is made that the scaling matrix, M, is symmetric. After assuming without loss of generality that the optimal M is actually positive semi-definite, the problem (20) can be equivalently formulated with a linearizing change of variables as

$$\sup_{Z \succeq 0, p} (\det Z)^{1/r} \text{ subject to:}$$
$$\|Zv_j - p\|_\infty \leq 1, \quad j = 1, \ldots, n \tag{23}$$

where r is the smallest integer such that $2^r \geq m$. This problem can be represented as a convex semi-definite program (SDP) using YALMIP [10] and solved using SDP solvers such as SeDuMi [11]. In the case when the

9

optimal Z is finite, any SDP solver is guaranteed to find the global minimum in polynomial time. Because the scalar characterization is a special case of this one, this optimization is guaranteed to give better results. Once the optimization has been solved for Z^* and p^*, the corresponding optimal values of M and $\bar{q}$ are recovered by

$$M^* = (Z^*)^{-1}$$
$$\bar{q}^* = M^* p^*$$
(24)

Dimensionality Reduction

In a physical system, it is likely that coupling exists among parameter variations such that they can be well-approximated using a reduced-order space. For example, it can be observed in Fig. 1 that the natural frequency in several modes increases as the associated damping increases. When using control design methodologies such as robust H_2 synthesis [12], in which the amount of computation required to design a controller increases drastically as the number of uncertain parameters increases, it is crucial to describe the uncertainty in a system using a minimum number of parameters.

To begin, define the vector of uncertain parameters as q' and its measurement vectors as y_j. In this framework, a cost function that quantifies how well a kth order subspace approximates the actual data is given by

$$J_k = \sqrt{\sum_{j=1}^{n} \|y_j - \hat{y}_j\|_2^2}$$
(25)

where $\hat{y}_j$ is the value of y_j after being translated and then projected onto a kth order subspace. The problem of finding the optimal translation and a basis for the optimal k^{th} order subspace under this cost function is equivalent to principal component analysis [13] and has a solution which is easy to compute. The optimal translation, $\bar{y}$ is given by the mean of the measurement vectors. Defining $w_j = y_j - \bar{y}$ and performing the singular value decomposition

$$\begin{bmatrix} w_1 & \cdots & w_n \end{bmatrix} = \sum_{i=1}^{p} \sigma_i \left(u_i v_i^T \right)$$
(26)

gives a value for $U_k = [u_1 \cdots u_k]$, whose columns form the basis of the optimal subspace. The corresponding optimal value of the cost function is

$$J_k^o = \sqrt{\sum_{i=k+1}^{p} \sigma_i^2}.$$
(27)

With this, the parameters which describe the location in the kth order subspace and the approximation of

original uncertain parameter vector are given respectively by

$$q'' = U_k^T (q' - \overline{y}) \tag{28}$$

$$\hat{q}' = U_k q'' + \overline{y}. \tag{29}$$

Methodology for Uncertainty Approximation

With the tools for uncertainty characterization and dimensionality reduction in place, it is possible to construct the following semi-automated methodology for uncertainty approximation in a system.

Initial Characterization

The vector of uncertain parameters, q, is first characterized using the scalar characterization, which gives values of $\overline{q}$ and M. The vectorial characterization is not used here because at this stage, the optimal Z in (23) for this set of uncertain parameters is often not finite.

Dimensionality Reduction

To nominalize the importance of each uncertain parameter, q' is chosen to be δ. The measurements of q' (i.e. δ) are given by

$$y_j = M^{-1} (v_j - \overline{q}) \tag{30}$$

The designer must now make a decision on how many parameters will be kept. Since there is a closed-form solution for the optimal cost as a function of the dimension of the reduced order space, a plot of this could aid the designer in this decision. Once this is done, dimensionality reduction gives values of $\overline{y}$ and U_k. This step optimally finds a reduced order space which approximates the uncertainty in the system.

Final Characterization

The vector of uncertain parameters in the new coordinates is now taken to be $q'' = U_k^T (q' - \overline{y})$, which has the measurement vectors

$$v_j'' = U_k^T (y_j - \overline{y}) \tag{31}$$

Due to the dimensionality reduction, the optimal Z in (23) must be finite. Thus, the vectorial characterization can be used to find values of $\overline{q}''$ and M'' so that $q'' = \overline{q}'' + M'' \delta''$. This step finds the best characterization of the reduced uncertain parameters subject to M being symmetric.
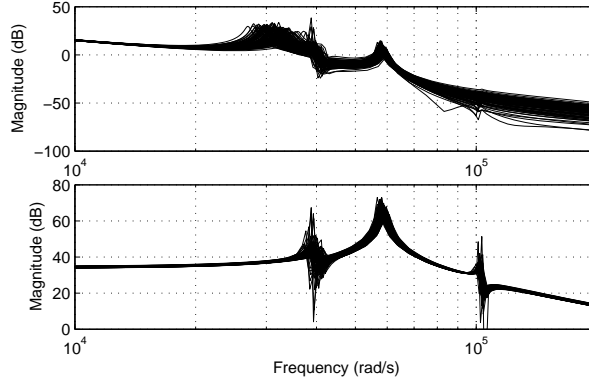
Figure 6: Bode magnitude plots of 100 random samples of the uncertain model characterized by the 14 uncertain parameters
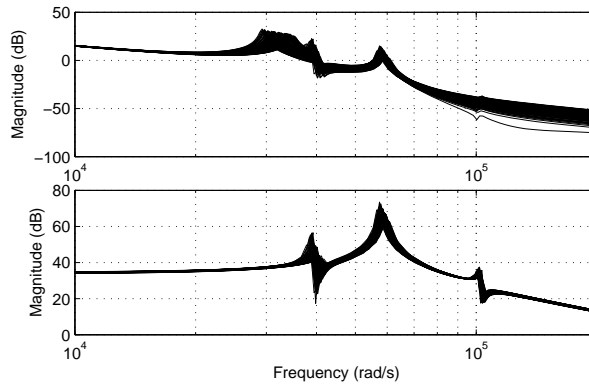

Figure 7: Bode magnitude plots of 100 random samples of the uncertain model characterized by 3 uncertain parameters

Substitution then gives the approximation of the parameter vector, $\hat{q}$, by

$$
\begin{aligned}
\hat{q} &= \overline{q} + M\left[U_k q'' + \overline{y}\right] \\
&= (\overline{q} + M\overline{y} + MU_k\overline{q}'') + MU_k M''\delta''
\end{aligned}
\tag{32}
$$

This characterization of the parametric uncertainty in the system is optimal in the sense that it minimizes the cost of the approximation, J_k, and also is minimally conservative with respect to q''. The only design decision is the choice of how many uncertain parameters to keep in the dimensionality reduction step. To understand the trade-off here, compare Fig. 6, in which the maximum number of uncertain parameters is kept, and Fig. 7, in which only 3 uncertain parameters are kept. Although keeping the maximum number of uncertain parameters ensures that all plant variations are exactly captured by the uncertainty description, it is also very conservative and will make the controller design process very computationally expensive. Thus, in addition to reducing the computation required to design a controller, reducing the number of uncertain parameters also reduces the conservatism of the uncertainty description.

12

Table 1: 2-norm error of models with reduced uncertainty description

Model Reduction	2-norm	
Technique	Mean	Standard Deviation
Data Fusion	6.7e4	4.6e4
BC Iteration	7.9e5	4.5e4

Comparison of Methods

This section compares the effectiveness of the uncertainty characterization using the two model reduction methods described in sections III and IV. The quality of the uncertainty model is evaluated by taking each of the plants in the set of reduced-order models and approximating the parameter vector by substituting v_j'' for q'' in (33). Then a 2-norm metric is used to quantify the error between each model and its approximated counterpart. Table 1 summarizes the resulting error. The results indicate that the final approximated uncertainty characterization is more complete when using the data fusion technique for model reduction. The likely reason is that the data fusion technique results in fewer initial uncertain entries in the state space matrices. Therefore, less information is lost when reducing to only three uncertain parameters. The tradeoff is that in the model reduction phase, the data fusion technique does not guarantee a minimized error between the full-order and reduced-order models.

Conclusion

This paper presented systematic algorithms that effectively reduce the model order and conservatism in a dynamic model of a HDD with parametric uncertainty. Order reduction of the MIMO model was addressed either by simultaneous fitting of multiple experimental data sets, or by a refined model truncation technique. While the former method results in fewer initial uncertain parameters, the latter provides a better match with the full-order model. Overall, the result is an uncertain state space model of manageable size to be used in robust H_2 controller synthesis.

Future work will involve demonstrating the use of the reduced order model in practical H_2 control synthesis applications. In addition, the algorithms will be modified to handle discrete-time models and stochastic distributions of uncertain parameters. The algorithms presented require a minimal amount of intuitive knowledge from the user, making them conducive to implementation in semi-automated software. Ultimately, the goal is a viable package that will facilitate system identification for uncertain systems, thus expanding the use of robust H_2 control design in the hard disk drive industry and in similar applications.

Acknowledgment

Bibliography

[1] Y. Li and R. Horowitz, "Design and testing of track following controllers for dual-stage servo systems with pzt-actuated suspensions," *Microsystems Technologies*, vol. 8, pp. 194-205, 2002.

[2] R. Horowitz, T.L. Chen, K. Oldham and Y. Li, "Design, Fabrication and Control of Micro-Actuators for Dual-Stage Servo Systems in Magnetic Disk Files," *Springer Handbook of Nanotechnology*, ed. B. Bushan, Springer, New York, January 2004.

[3] X. Huang, R. Nagamune and R. Horowitz, "A Comparison of Multirate Robust Track-Following Control Synthesis Techniques for Dual-Stage and Multi-Sensing Servo Systems in Hard Disk Drives," *IEEE Trans. on Magnetics*, vol.42, no.7, pp. 1896-904, July 2006.

[4] R. de Callafon, R. Nagamune and R. Horowitz, "Robust Dynamic Modeling and Control of Dual-Stage Actuators," *IEEE Trans. on Magnetics*, vol.42, no.2, pp. 247-54, Feb. 2006.

[5] K. Oldham, S. Kon, and R. Horowitz, "Fabrication and optimal strain sensor placement in an instrumented disk drive suspension for vibration suppression," *Proceedings of the 2004 American Control Conference IEEE*, vol.2, pp. 1855-61, Piscataway, NJ, USA, 2004.

[6] D.J. Ewins, *Modal testing: Theory and practice.* J. Wiley & Sons, New York, 1986.

[7] J.R. Taylor, *An Introduction to Error Analysis.* University Science Books, Mill Valley, CA, USA, 1982.

[8] K. Zhou and J. Doyle, *Essentials of Robust Control.* Prentice Hall, Upper Saddle River, New Jersey, USA, 1998.

[9] W. Yan and J. Lam, "Approximate approach to H2 optimal model reduction," *IEEE Transactions on Automatic Control*, vol.44, no.7, pp. 1341-1358, Jul. 1999.

[10] J. Löfberg, "YALMIP : A toolbox for modeling and optimization in MATLAB," In *Proceedings of the CACSD Conference*, Taipei, Taiwan, 2004. Available from http://control.ee.ethz.ch/joloef/yalmip.php.

[11] J.F. Sturm, "Using SeDuMi 1.02, a matlab toolbox for optimization over symmetric cones," *Optimization Methods and Software*, vol.11-12, pp. 625-653, 1999. Special issue on Interior Point Methods.

[12] R. Nagamune, X. Huang, and R. Horowitz, "Multi-rate track-following control with robust stability for a dual-stage multi-sensing servo system in HDDs," *Proc. of the Joint 44th IEEE Conference on Decision and Control* and *European Control Conference ECC 2005*, pp. 3886-3891, Seville, Spain, Dec. 2005.

[13] I. Jolliffe, *Principle Component Analysis*. Springer-Verlag, New York, 1986.